Evolution microstructurale en soudage par friction malaxage – Application à la prédiction des propriétés mécaniques

V. Legrand,
G. Guillemot, Ch.-A. Gandin

CEMEF – Mines ParisTech,
Sophia Antipolis, France

MINES ParisTech

14EME COLLOQUE 'MODÉLISATION ET SIMULATION NUMÉRIQUE DU SOUDAGE' - 17 MARS 2016
'COMMENT LES MODÈLES ET LEURS CARACTÉRISATIONS EXPÉRIMENTALES INFLUENCENT LES RÉSULTATS D'UNE SIMULATION NUMÉRIQUE'

Introduction / FSW processes

❑ Current riveting process

Riveting in Aircraft Industries

→ Overweight
→ Defects
→ Cost in material
→ Time of assembly

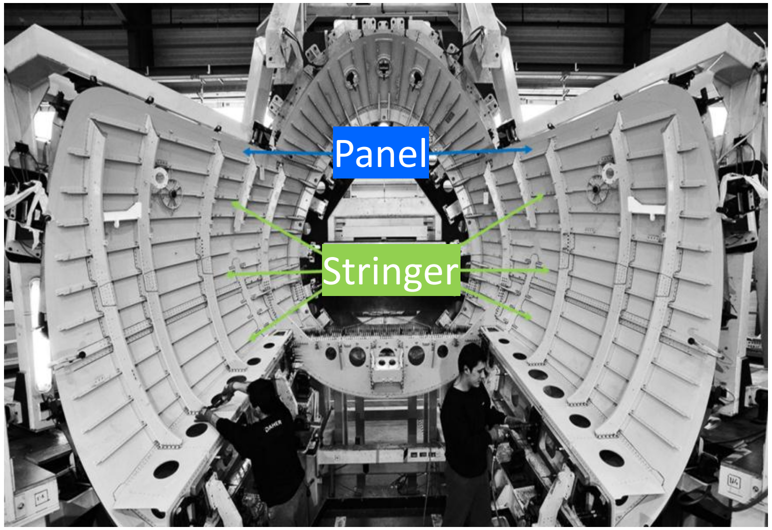

Aircraft fuselage / Panels and Stringers of A340

❑ Optimize assembly of fuselage

❑ FSW process as an alternative to riveting

❑ Advantages of FSW process

- Welding of heterogeneous material (AA2024 – panel / AA7175 – stringer)
- Mushy state / No remelting => no damage on materials properties
- Improvement of the tensile strength of the assembly vs. riveting process

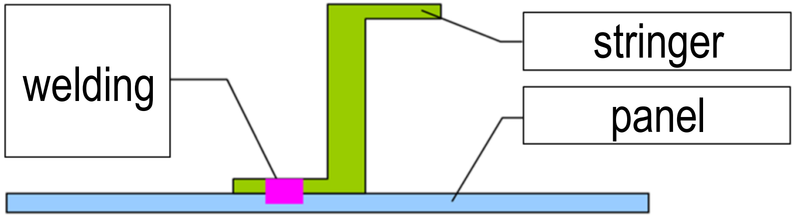

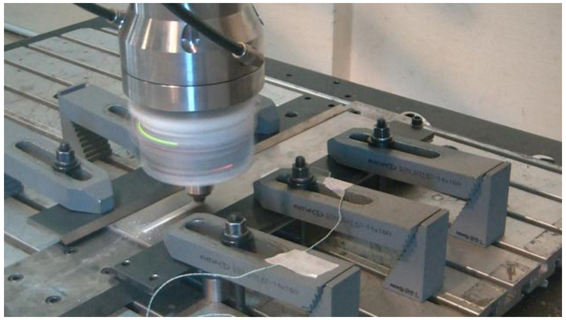

Macroscopic modelling / Approach

- **Development of a thermo-mechanical modelling for FSW processes**
  - Prediction of defects development in FSW processes
  - Cavities in the back part of the pin / Surface defects

Complex geometry
+
Mesh evolution
=
Arbitrary **L**agrangian -**E**ulerian approach (**ALE**) [1,2]

- **Thermomechanical resolution [3]**
  - Mushy state close to the tool
  - Perfectly viscoplastic solid
  - Norton-Hoff constitutive model

$$\bar{\sigma} = \sqrt{3}\,K(T)(\sqrt{3}\dot{\bar{\varepsilon}})^{m(T)}$$

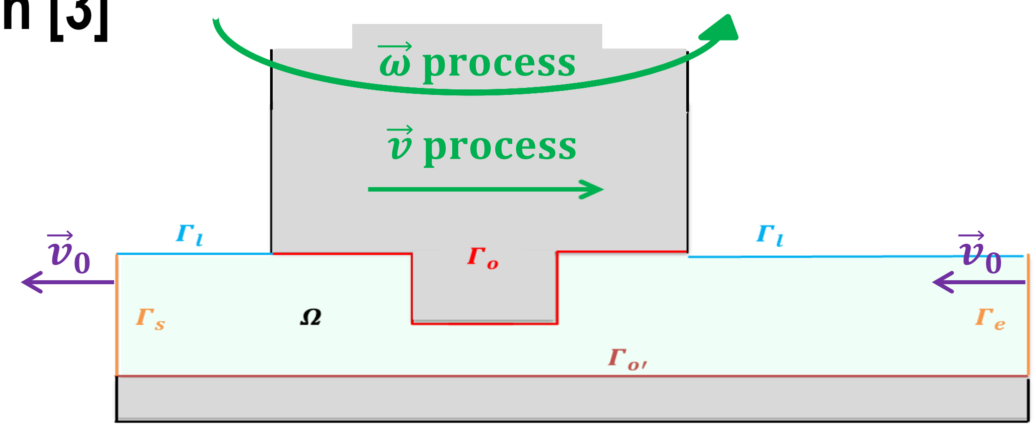

[1] H. Schmidt, J. Hattel, Modelling Simul. Mater. Sci. Eng., 13 (2005), 77
[2] S. Guerdoux, L. Fourment, Modelling Simul. Mater. Sci. Eng., 17 (2009)
[3] S. Gastebois, *Simulation numérique 3D du FSW à l'aide d'une formulation ALE*, Doctorat Mines Paristech, 2015

Macroscopic modelling / Evolution

❑ Macroscopic simulation

- Predict default occurrences to choose ideal parameters
- Define thermal evolution while welding

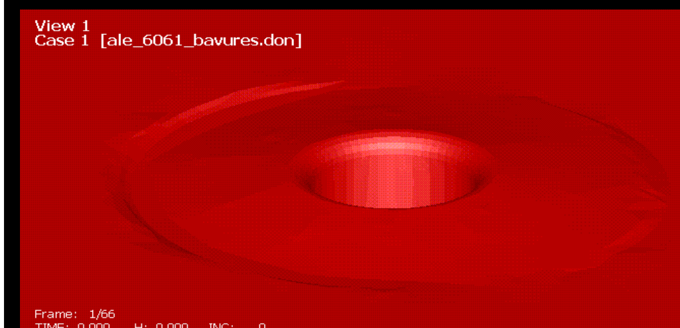

Flash

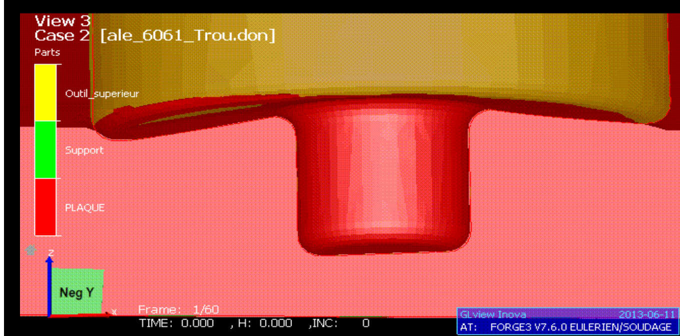

Tunnel hole

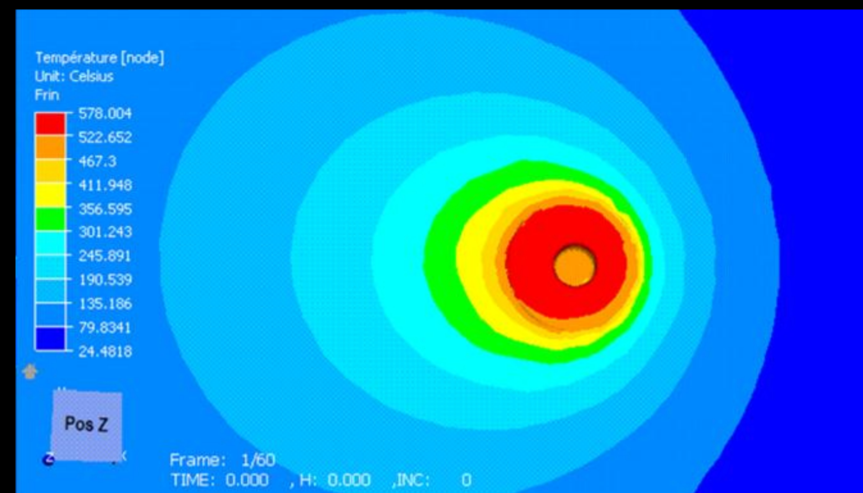

Thermal Evolution

FORGE HPC•2011 TRANSVALOR

[3] S. Gastebois, *Simulation numérique 3D du FSW à l'aide d'une formulation ALE*, Doctorat Mines Paristech, 2015

❑ Precipitation evolution modelling

- ❑ Precipitate size distribution (PSD) [4] model for multiphase system
- ❑ Modelling of the nucleation, growth and coarsening processes during the whole FSW process
- ❑ Coupling with macroscopic temperature evolution (Forge®) (thermal history of domain)
- ❑ Coupling with the Thermocalc (TCAL3) database for phase equilibrium computations and chemical diffusivities
- ❑ Hardness profile prediction in HAZ, TMAZ and Nugget after FSW

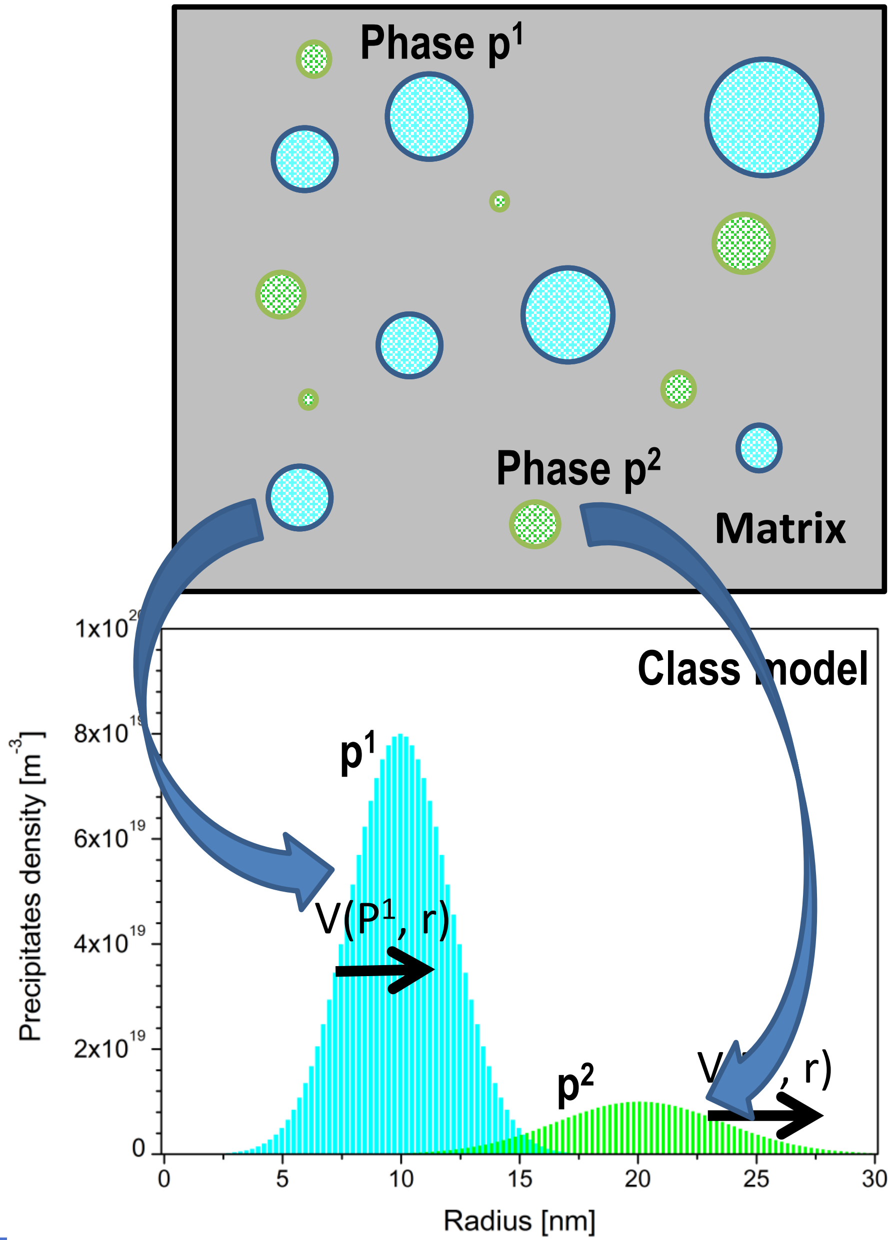

[4] O.R. Myhr and O. Grong, Acta Materialia, 48 (2000), 1605

Microscopic modelling / Algorithm

❑ Precipitation evolution modelling

- ❑ **Nucleation** of new precipitates depending from local composition & temperature
- ❑ Computation of spherical precipitates **growth** kinetics coupled with Thermocalc
- ❑ Resolution of the **density distribution** conservation equation depending from computed velocity in each class
- ❑ Computation of the **volume fraction** of precipitate for hardness prediction
- ❑ Solute conservation equation resolution for average **matrix** [FCC_A1] **composition** computation

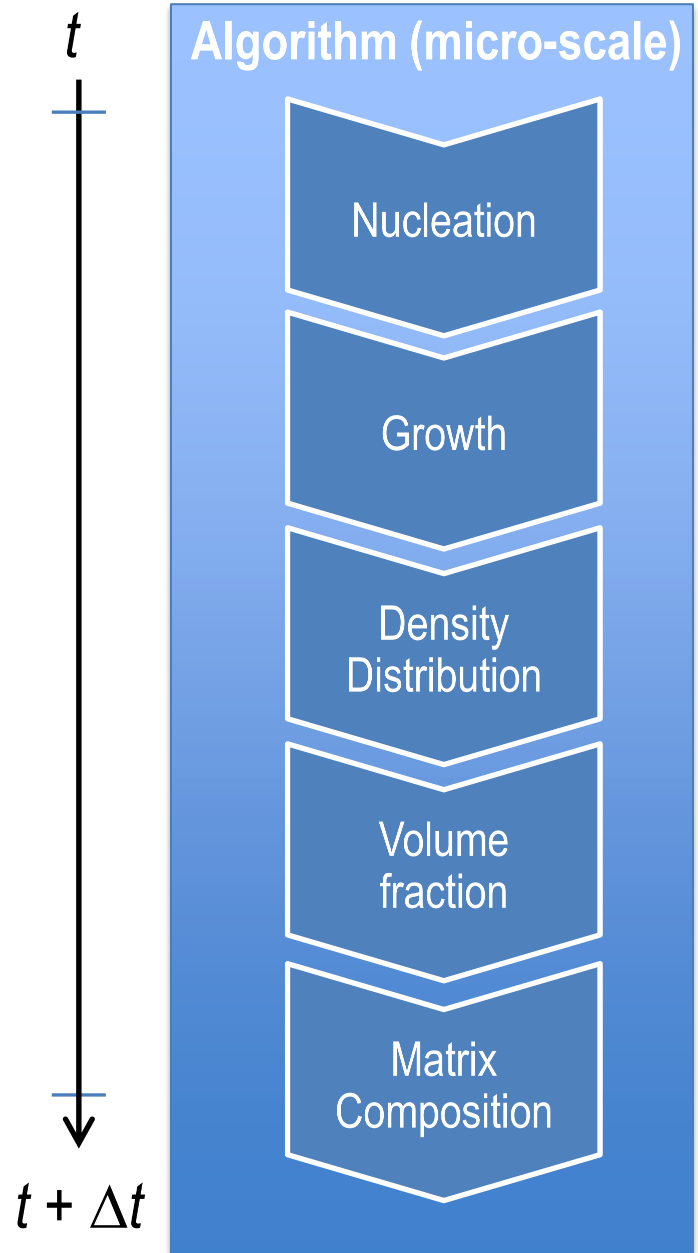

Nucleation

- Computation of the Gibbs energy associated to precipitate nucleation

$$\Delta G_v^p = \frac{R_g.T}{V_m^p}\left[\sum_{i=1}^{N} X_i^p.\ln\left(\frac{X_i^m}{X_{eq,i}^m}\right)\right]$$

(diluted ideal solution)

- Critical radius of nucleation

$$R^* = \frac{2\ \gamma^{m/p}}{\Delta G_v^p}$$

- Velocity of precipitate nucleation

$$J_s = Z\beta(N_{tot} - N)exp\left(-\frac{\Delta G^*}{k_B T}\right)$$

Z : Zeldovich factor / β : rate of cluster growth

N_{tot} : Maximal number of nucleation sites

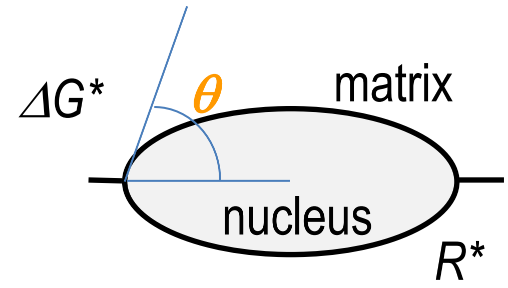

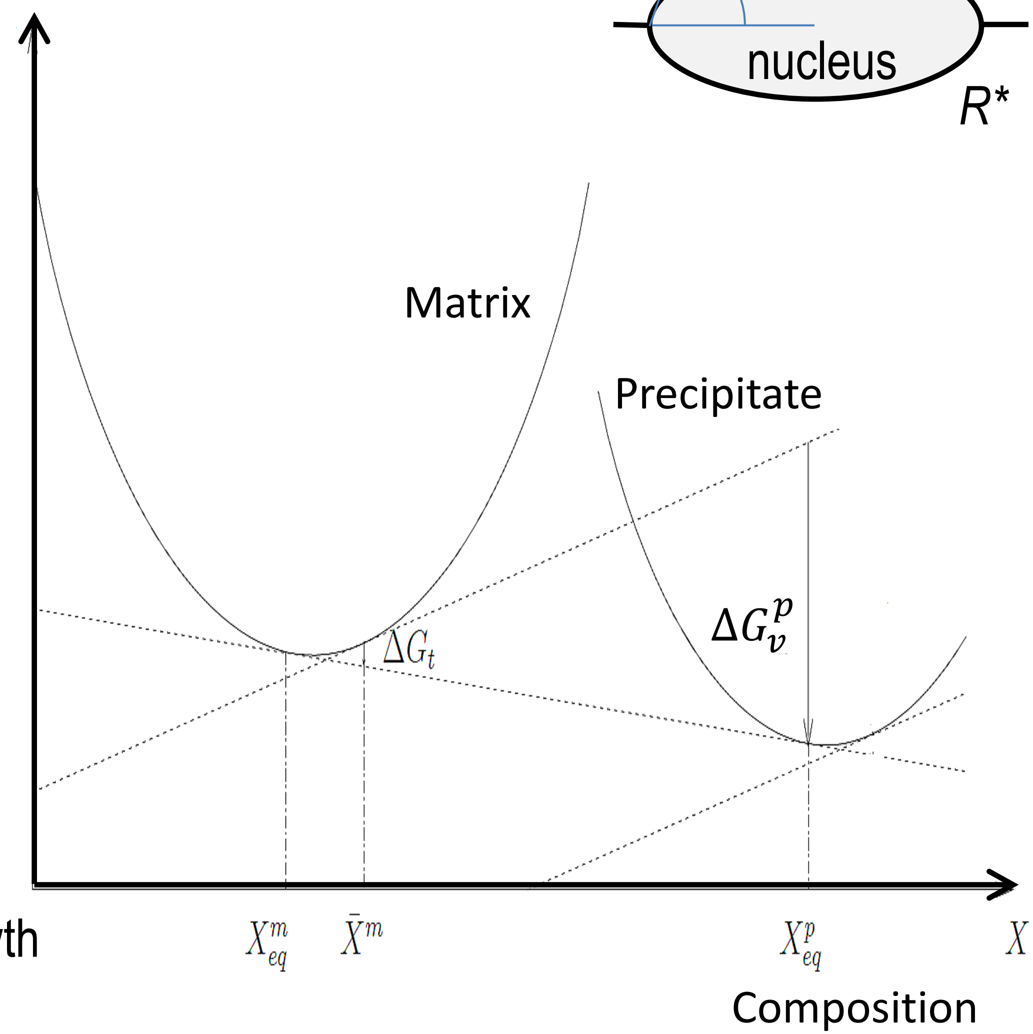

Growth kinetics computation

- Computation of the critical radius, R* for each phase
  - r > R* ⇒ **Growth**
  - r < R* ⇒ **Dissolution**

- Kinetics computation depending from growing regime
  - **Growth** / Aaron (exact) [5,6] :

$$\Omega_i = \frac{x_i^2}{2}\left[1 - \frac{x_i}{2}\sqrt{\pi}\exp\left(\frac{x_i^2}{2}\right) erfc\left(\frac{x_i}{2}\right)\right] \text{ with } x_i = \sqrt{\frac{2rv}{D_i}}$$

  - **Dissolution** / Laplace (approximation) :

$$\Omega_i = \frac{r\,v}{D_i}$$

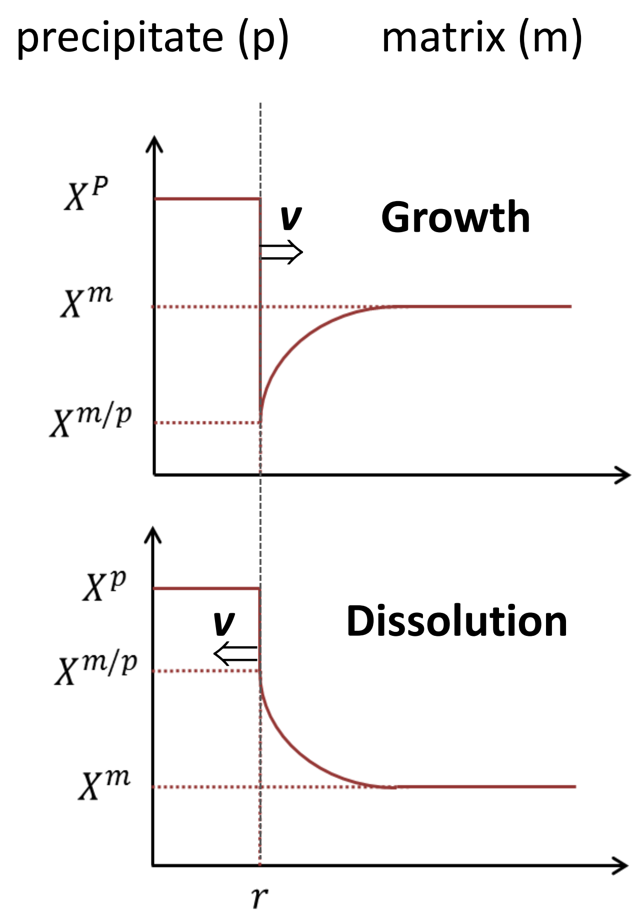

Solved with respect of the thermodynamical equilibrium at *m/p* interface: $K_{eq}(T,r) = \prod_{i=1}^{N} X_i^{m/p\,X_i^p}$

[5] H.B. Aaron, D. Fainstein, G.R. Kotler, J. Appl. Phys. 11 (1970) 4404
[6] G. Guillemot, Ch.A. Gandin, Acta materialia, 97 (2015), 419]

Microscopic modelling / Density

❑ Density distribution conservation equation

- ❑ Conservation of the precipitate density

$$\frac{\partial N}{\partial t} = -\frac{\partial (Nv)}{\partial r} + S$$

- ❑ Discretized approach for the resolution

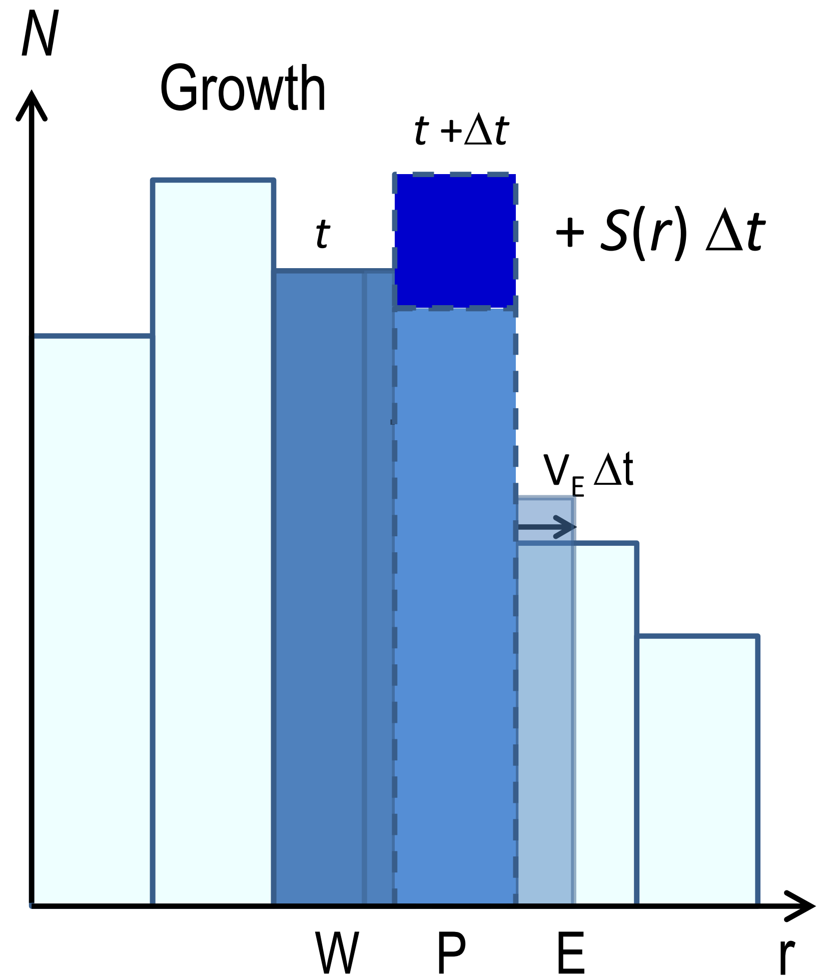

$$\left(N_P^t - N_P^{t-\Delta t}\right)\frac{\Delta R}{\Delta t} =$$

[W → P] $\left[N_W^t max(v_W^t, 0) - N_P^t max(-v_W^t, 0)\right]$

[E → P] $-\left[N_P^t max(v_E^t, 0) - N_E^t max(-v_E^t, 0)\right]$

[nucl. in R* class] $+S\Delta R$

$$a_{k-1}^t N_{k-1}^t + a_k^t N_k^t + a_{k+1}^t N_{k+1}^t = b^{t-\Delta t}$$

Matrix resolution / Update of precipitate density distribution, *N* à *t*+Δ*t*

Microscopic modelling / Hardness

- **Mechanical properties evolution**
  - Additional yield strength / contributions
    - Matrix composition changes
    - Precipitate distribution
  - Solid solution contribution

$$\sigma_{SS} = 26\left(X_{Cu} + X_{Mg}\right)^{3/2}$$

  - Cross-mechanism contribution, depending from the threshold precipitate radius, r_C

$$r < r_c \Rightarrow \qquad \sigma_S = 0.7 M \alpha^{3/2} \mu \sqrt{\frac{rg}{b}}$$

$$r > r_c \Rightarrow \qquad \sigma_P = K\mu \frac{b}{r}\sqrt{g}$$

M : Taylor factor, b : burgers vector,
μ : shear modulus, g : fraction

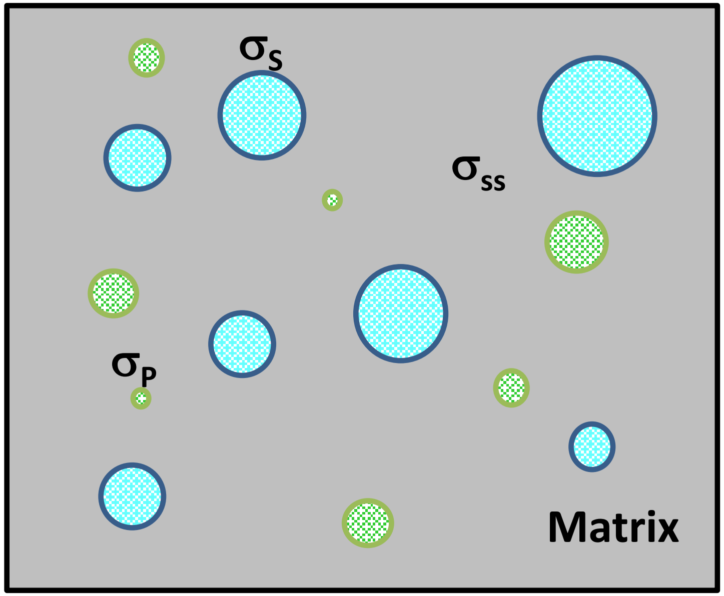

$$\sigma_Y = 52 + \sigma_{SS} + \sqrt{\sum_{\varphi}\left(\sum_{r<r_c}\sigma_S{}^2 + \sum_{r>r_c}\sigma_P{}^2\right)}$$

(Yield strength)

$$\mathrm{HV} = c\,\sigma_Y + d$$

(Hardness)

Microscopic modelling / Calibration

❑ Non-isothermal calibration

- ❑ AA2024-T3 in delivery state (*e* = 2.5 mm)

	Al	Cu	Fe	Mg	Mn
%at.	Balance	3.42	0.06	1.76	0.4

(*EDS analysis – ⟨matrix + precipitate⟩*)

- ❑ Two hardening phases are considered:
  - ❑ GPB zone (dissolution)
  - ❑ S phase (precipitation)
- ❑ DSC analysis for two heating rates
- ❑ Calibration of N_{tot}, θ, $\gamma^{m/p}$ parameters

	GPB zones	S phase
Nucleation site density, N_{tot} [m^{-3}]	10^{26}	5.10^{23}
Wetting angle, θ [°]	30	40
Interfacial energy, $\gamma^{m/p}$ [$mJ \cdot m^{-2}$]	100	125

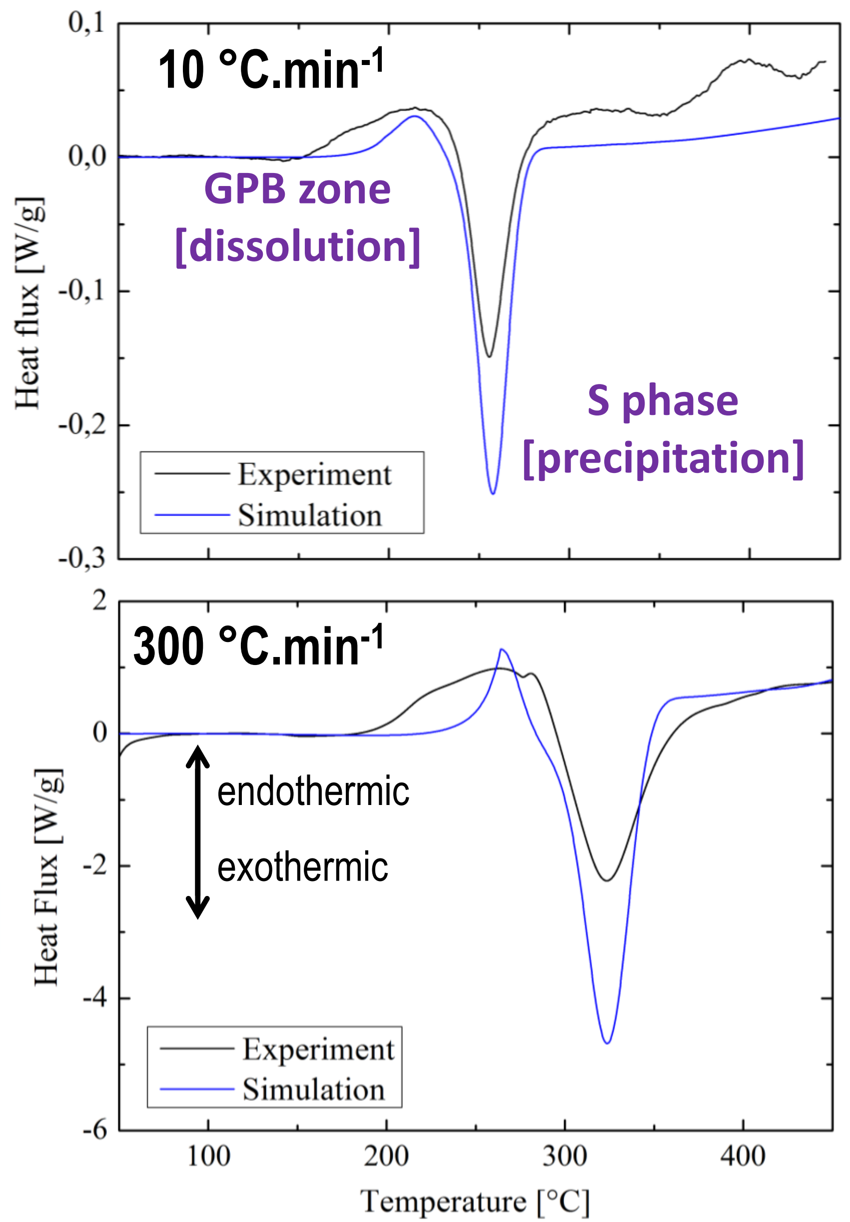

Isothermal calibration

- Calibration of mechanical properties as a function of precipitates distribution for both hardening phases
- DSC analysis developed on heat treated samples for different time duration at *T* = 190 ºC
- Precipitation evolves showing a decrease of dissolved GPB zone [A] and an increase of formed S phase [B] due to the evolution of the initial amount of the two phases

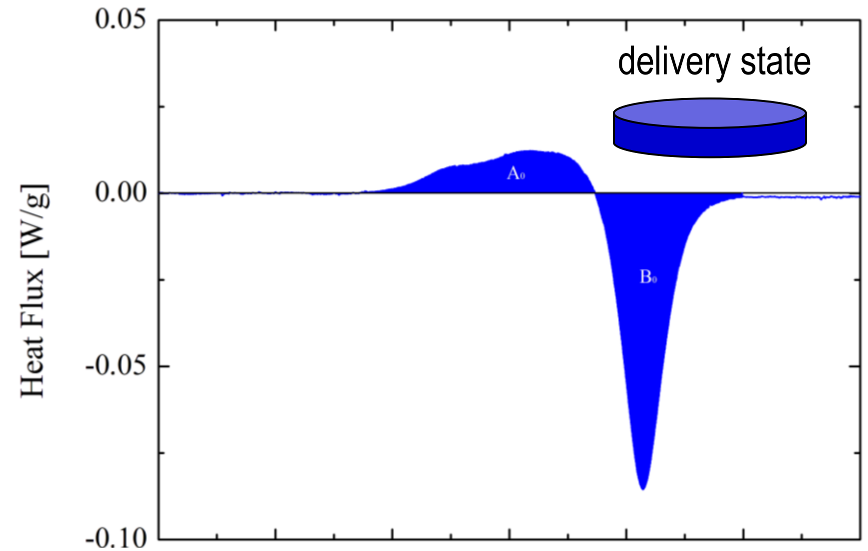

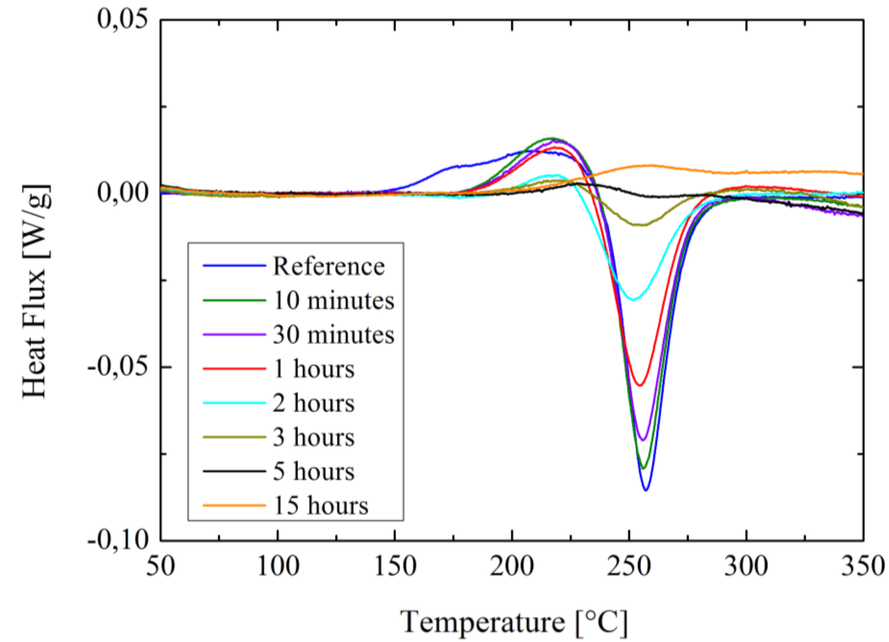

Microscopic modelling / Calibration

❑ Isothermal calibration

- ❑ Time evolution of phase fractions during heat treatment shows the progressive changes of the system
- ❑ Simulations are shown in accordance with experiments for the prediction of the evolution for both GPB zone and S phase
- ❑ Measured hardness on quenched samples are compared to the mechanical modelling, based on corresponding precipitate distribution

M [-]	α [-]	μ [Pa]	b [nm]	K [-]	c [HV·MPa^{-1}]	d [HV]
3	**0.038**	25000	0.3	**1.06**	**0.26**	**62.23**

Estimate mechanical coefficients

[6] C. Genevois C, PhD Thesis, INP Grenoble, 2004

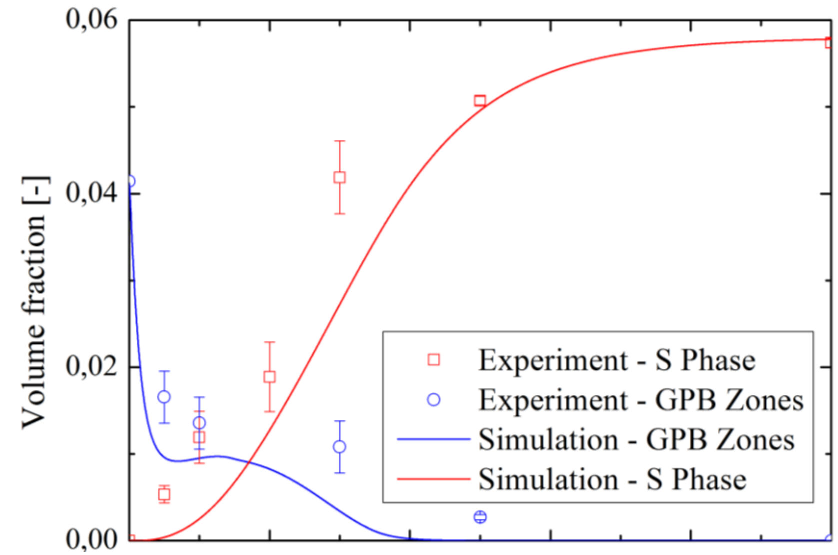

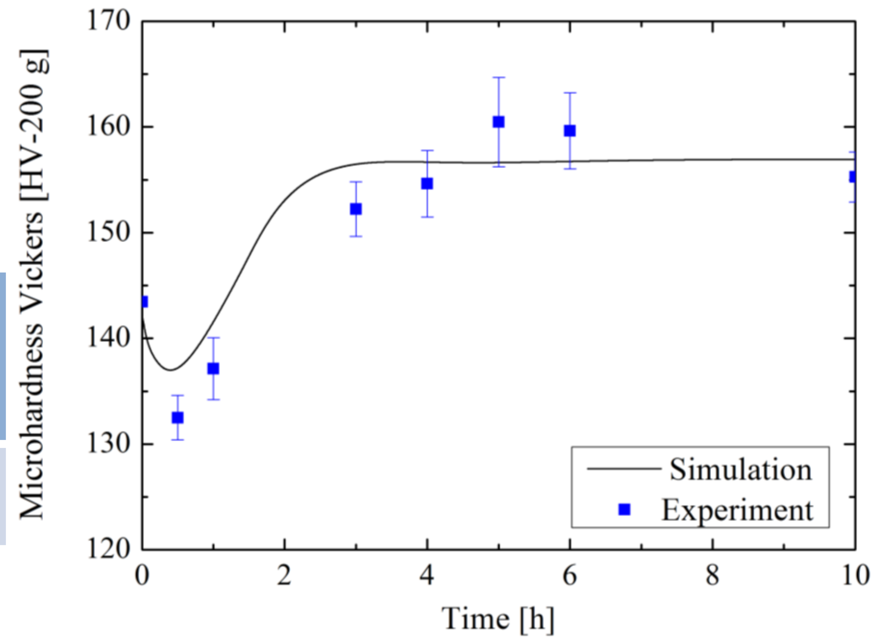

FSW experiment

- **Mechanical deformation of a FSW weld**
  - Uniaxial tensile test : Localization of the deformation
  - Hardness profile influence

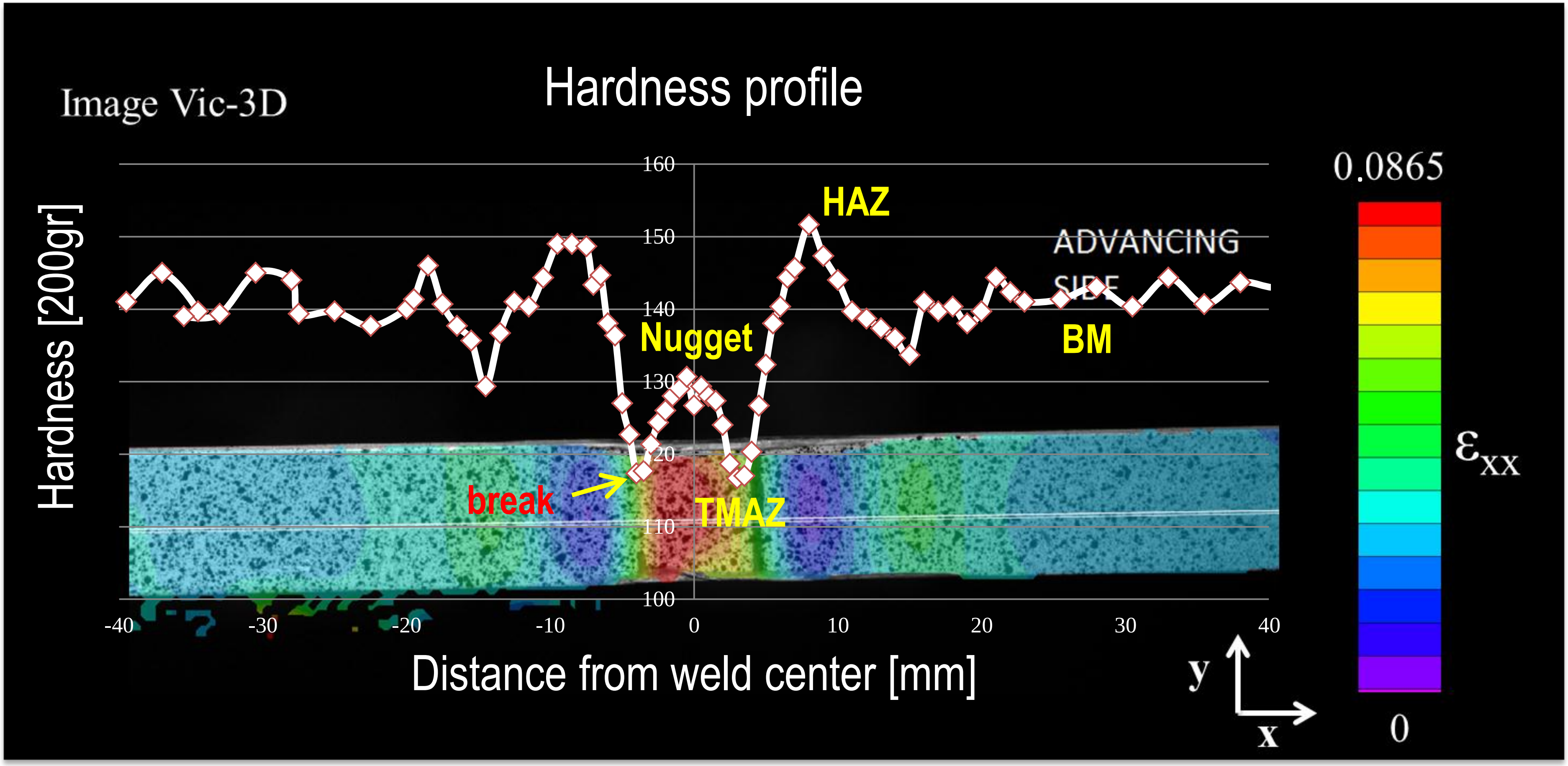

FSW Analysis

- **Precipitate evolution in FSW proces**
  - FSW instrumented equipment used to develop linear welding in controlled condition [*V*, *W*, *F*]
  - DSC Analysis conducted on specific welding condition with samples cut in a cross section of welded pieces
  - Evolution of the signal induced by GPB zone and S phase evolution due to thermal evolution induced by FSW process
  - Dependence of the amount of GPB zones and S phase with position in the weld are measured
  - Decrease of GPB zones and increase of S phase in TMAZ are well reproduced as well as S phase development in nugget

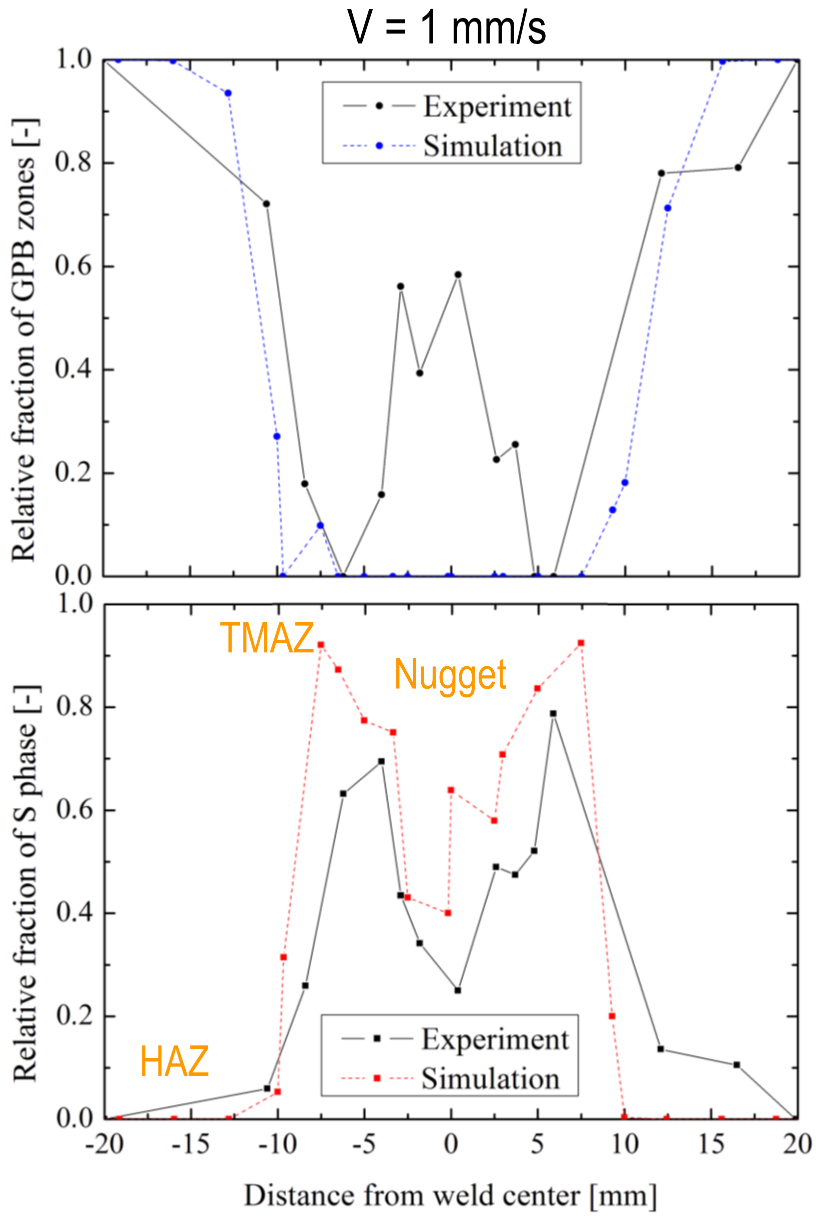

FSW Analysis

- Hardness profile evolution
  - Hardness measurements are conducted for different welding velocities for similar forces and rotational velocity
  - Experiment
    - Similar profiles are observed with a decrease in the range of hardness evolution for the largest velocity.
    - Heterogeneity are less visible and the length of the weld domain decreases
  - Simulation
    - Reproduces the hardness profile evolution based on Forge® simulations [temperature]
    - Increase of hardness in the nugget domain is not visible (no simulation of natural ageing / i.e. GPB Zone development)

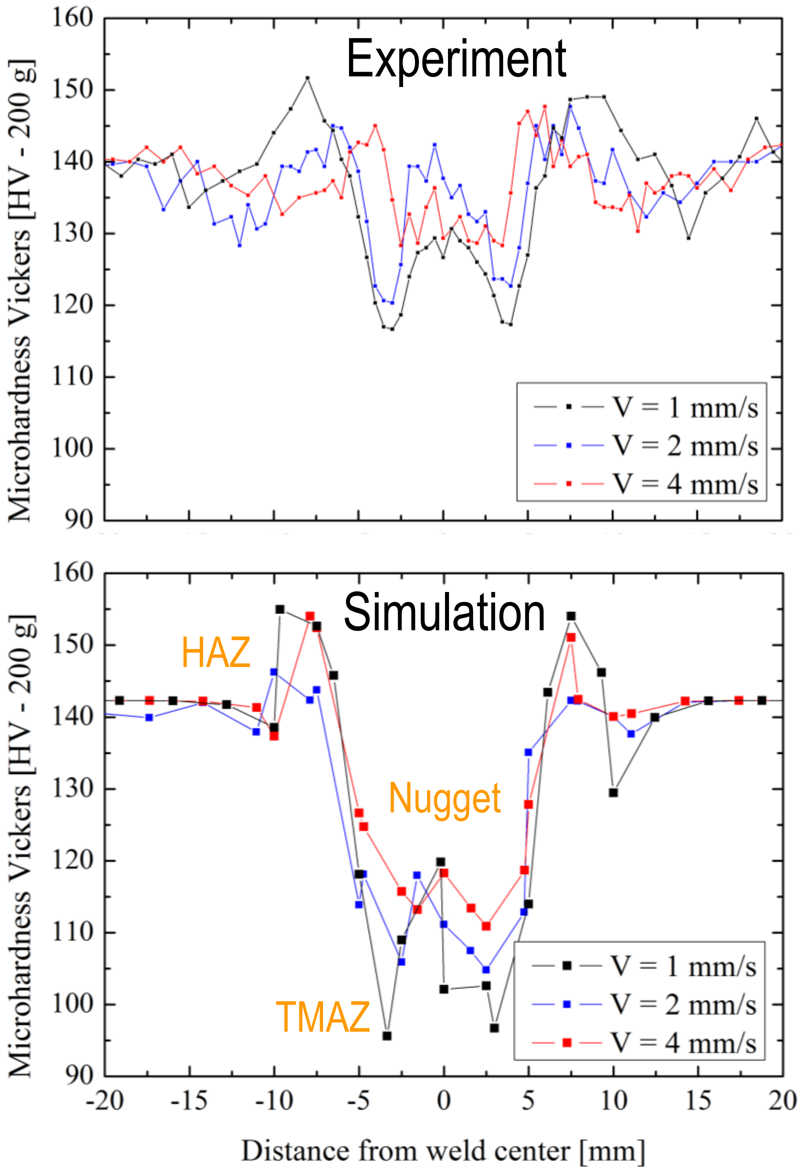

Conclusions

- An efficient class model is developed in order to **simulate multi-phases precipitation considering nucleation, growth and coarsening steps** in a single approach **coupled with thermodynamic database**

- Precipitate evolution during FSW process on AA2024 aluminium alloy is conducted with **temperature evolution deduced from macroscopic simulations**, developed in a thermomechanical modelling (Forge® software)

- **Final heterogeneous mechanical properties are computed** for the different weld domains from precipitate size distribution, after calibration conducted on isothermal tests

- **Experiments and simulation shows similar evolution with comparable final mechanical properties**. Future experiments will be conducted in order to improve the estimation of final precipitate size distribution and related properties, considering natural ageing at ambient temperature.

Questions ?

MINES ParisTech

Cemef
CENTRE DE MISE EN FORME DES MATERIAUX